

Holographic Entanglement Negativity for Adjacent Subsystems in AdS_{d+1}/CFT_d

Parul Jain^{*1,2,3}, Vinay Malvimat^{†3}, Sayid Mondal^{‡3}, and Gautam Sengupta^{§3}

¹Dipartimento di Fisica, Università di Cagliari, Cittadella Universitaria, 09042 Monserrato, Italy

²INFN, Sezione di Cagliari, Italy

³Department of Physics,
Indian Institute of Technology,
Kanpur, 208016,
India

December 14, 2024

Abstract

We propose a holographic conjecture for the entanglement negativity between two adjacent subsystems characterizing a mixed state in a boundary conformal field theory through the AdS_{d+1}/CFT_d correspondence. This involves an algebraic sum of the areas of bulk co-dimension two extremal surfaces which reduces to the holographic mutual information. We employ our conjecture to compute the holographic entanglement negativity for subsystems of rectangular strip geometries both at zero and finite temperatures from the dual bulk AdS_{d+1} vacuum and the AdS_{d+1} -Schwarzschild black hole.

^{*}E-mail: parul.jain@ca.infn.it

[†]E-mail: vinaymm@iitk.ac.in

[‡]E-mail: sayidphy@iitk.ac.in

[§]E-mail: sengupta@iitk.ac.in

Contents

1	Introduction	2
2	Entanglement negativity in CFT_{1+1}	3
2.1	Entanglement negativity for two adjacent intervals in vacuum	3
2.2	Entanglement negativity for two adjacent intervals at finite temperature	4
3	Holographic entanglement negativity for $\text{AdS}_{d+1}/\text{CFT}_d$	5
4	Holographic entanglement negativity for $\text{AdS}_{d+1}/\text{CFT}_d$ in vacuum	5
5	Holographic entanglement negativity for $\text{AdS}_{d+1}/\text{CFT}_d$ at finite temperature	6
5.1	Entanglement negativity in the low temperature limit	7
5.2	Entanglement negativity in the high temperature limit	8
6	Summary and conclusions	10
7	Acknowledgment	10

1 Introduction

Quantum entanglement has developed into an ubiquitous feature of modern fundamental physics in recent times connecting a spectrum of diverse areas from quantum information theory to quantum gravity. In this regard entanglement entropy has evolved as the most significant and convenient measure to characterize the entanglement of a bipartite quantum system in a pure state. From quantum information theory this is defined as the von Neumann entropy of the reduced density matrix of the corresponding subsystem. For $(1+1)$ -dimensional conformal field theories (CFT_{1+1}) the entanglement entropy may be computed through the *replica technique* developed by Calabrese et al in [1, 2].

In the context of the AdS/CFT Ryu and Takayanagi in [3, 4] proposed a geometric prescription for the entanglement entropy of holographic CFTs. For a subsystem described by a spatial region A on the boundary the entanglement entropy is given from this conjecture by the area of the co-dimension two bulk AdS_{d+1} extremal surface anchored on the region A . In the recent past this has led to intense research activity into entanglement issues for diverse holographic CFTs both at zero and finite temperatures [5–11].

Despite the crucial role of entanglement entropy in the characterization of pure state entanglement it was inadequate as an entanglement measure for mixed quantum states. This was an unresolved issue in quantum information theory and in a seminal work Vidal and Werner [12] introduced the quantity termed *entanglement negativity* as a computable measure for the upper bound on the distillable entanglement in mixed states. The non convexity for this measure was established in [13]. Interestingly the authors in [14–16] computed this quantity in CFT_{1+1} employing a variant of the usual replica technique involving a certain four point function of the twist/anti-twist operators.

Naturally it was critical to establish a holographic description for the entanglement negativity of boundary CFTs in terms of the bulk geometry in the AdS/CFT scenario. In spite of interesting insights in [17, 18], a clear holographic prescription for the entanglement negativity of CFTs remained an unresolved issue. Two of the present authors (VM and GS) in the articles [19–21] (*CMS*) proposed a holographic conjecture for the entanglement negativity of such boundary CFT_d s which exactly reproduced the CFT_{1+1} [16] results in the large central charge limit.

It is important to emphasize that the *CMS* conjecture mentioned above refers to the entanglement negativity of a single subsystem within an infinite system described by the boundary CFT_d . In the articles [15, 16], the authors computed the entanglement negativity of a mixed state characterized by two finite intervals A_1 and A_2 in a CFT_{1+1} both at zero and finite temperatures. In a recent communication [22] the present authors established an independent holographic conjecture to compute the entanglement negativity between the two intervals mentioned above in the context of AdS_3/CFT_2 . It could be shown there that the corresponding entanglement negativity was characterized by a certain algebraic sum of the geodesic lengths in the bulk AdS_3 space time anchored on the two intervals, which reduced to the holographic mutual information. Remarkably the holographic entanglement negativity computed from the above prescription exactly reproduced the CFT_{1+1} results both for zero and finite temperatures in the large central charge limit [15, 23]. The holographic conjecture for the entanglement negativity [22] alluded above allowed a direct generalization to the AdS_{d+1}/CFT_d scenario. In this case the entanglement negativity could be characterized in terms of an algebraic sum of the areas of bulk extremal co dimension two surfaces anchored on the respective subsystems in the boundary CFT_d . As earlier this reduces to the holographic mutual information between the subsystems.

In this article we examine this critical issue and compute the holographic entanglement negativity of the mixed state described by two adjacent subsystems in the boundary CFT_d employing our conjecture. To this end we consider two adjacent subsystems A_1 and A_2 characterized by rectangular strip geometries and compute the corresponding holographic entanglement negativity both for zero and finite temperatures. For zero temperature the bulk configuration is described by the AdS_{d+1} vacuum whereas the finite temperature scenario is described by the AdS_{d+1} -Schwarzschild black hole. For the finite temperature case the computation of the holographic entanglement negativity required both a low and a high temperature approximations for the areas of the corresponding bulk extremal surfaces. At low temperatures the leading contribution arises from the AdS_{d+1} vacuum corrected by subleading thermal contributions. Interestingly for the high temperature case on the other hand the thermal contribution are precisely subtracted out. Hence at the leading order the entanglement negativity at high temperature is characterized by the area of the entangling surface on the boundary.

This article is organized as follows, in section 2 we briefly review the computation of the holographic entanglement negativity of two adjacent intervals in the AdS_3/CFT_2 scenario described in [22]. In section 3 we establish the corresponding holographic conjecture for the entanglement negativity of two adjacent subsystems in the context of the AdS_{d+1}/CFT_d correspondence. In the subsequent section 4 we

employ our conjecture to compute the holographic entanglement negativity for two adjacent subsystems of rectangular strip geometries at zero temperature from the bulk AdS_{d+1} vacuum. In section 5 we describe the corresponding computation for the finite temperature scenario from a bulk AdS_{d+1} -Schwarzschild black hole. In the final section 6 we summarize our results and present our conclusions and future open issues.

2 Entanglement negativity in CFT_{1+1}

In this section, we present a brisk review of *entanglement negativity* in CFT_{1+1} [14, 15]. To this end we consider a spatial tripartition of the CFT_{1+1} described by the intervals A_1 , A_2 and B with $A = A_1 \cup A_2 = [u_1, v_1] \cup [u_2, v_2]$ consists of two finite intervals A_1 and A_2 of length l_1 and l_2 respectively and $B = A^c$ represents the rest of the system. The reduced density matrix of the subsystem A is defined as $\rho_A = \text{Tr}_B \rho$ and $\rho_A^{T_2}$ is the partial transpose of the reduced density matrix. The entanglement negativity \mathcal{E} is defined as the logarithm of the trace norm of the partially transposed reduced density matrix [12], which is expressed as

$$\mathcal{E} = \ln \text{Tr} |\rho_A^{T_2}|. \quad (2.1)$$

The entanglement negativity may now be obtained through a replica technique as discussed in [14, 15] to determine $\text{Tr} (\rho_A^{T_2})^{n_e}$ and the replica limit is given as the analytic continuation of n_e through even sequences to $n_e \rightarrow 1$. This leads to the following expression for the entanglement negativity

$$\mathcal{E} = \lim_{n_e \rightarrow 1} \ln \text{Tr} (\rho_A^{T_2})^{n_e}. \quad (2.2)$$

For the mixed state described by the two intervals as shown in Fig. (1), the quantity $\text{Tr} (\rho_A^{T_2})^{n_e}$ is given by a four point function of the twist operators on the complex plane as follows

$$\text{Tr} (\rho_A^{T_2})^{n_e} = \langle \mathcal{T}_{n_e}(u_1) \overline{\mathcal{T}}_{n_e}(v_1) \overline{\mathcal{T}}_{n_e}(u_2) \mathcal{T}_{n_e}(v_2) \rangle_{\mathbb{C}}. \quad (2.3)$$

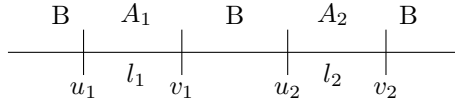


Figure 1: Schematic of two disjoint intervals A_1 and A_2 in a $(1+1)$ -dimensional boundary CFT.

2.1 Entanglement negativity for two adjacent intervals in vacuum

Here we briefly review the computation for the entanglement negativity of two adjacent intervals in a CFT_{1+1} at zero temperature [14, 15] and the corresponding holographic description in [22]. The related configuration may now be obtained by setting $v_1 \rightarrow u_2$ with $u_2 = 0$, $u_1 = -l_1$ and $v_2 = l_2$ as shown in Fig. (2) described below.

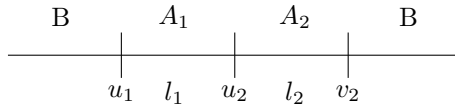


Figure 2: Schematic of two adjacent intervals A_1 and A_2 in a $(1+1)$ -dimensional CFT.

The quantity $\text{Tr} (\rho_A^{T_2})^{n_e}$ in the Eq. (2.3) for the two adjacent intervals is now described by a three point function of the twist operators as follows

$$\text{Tr} (\rho_A^{T_2})^{n_e} = \langle \mathcal{T}_{n_e}(-l_1) \overline{\mathcal{T}}_{n_e}^2(0) \mathcal{T}_{n_e}(l_2) \rangle. \quad (2.4)$$

The replica limit $n_e \rightarrow 1$ on Eq. (2.4) now leads to the following expression for the entanglement negativity

$$\mathcal{E} = \frac{c}{4} \ln \left(\frac{l_1 l_2}{(l_1 + l_2)a} \right) + \text{const}, \quad (2.5)$$

where a is the UV cutoff for the CFT . The ‘const’ term in the above expression may be neglected in the large central charge limit [22, 23].

In [22] the present authors proposed a holographic conjecture for the entanglement negativity of the configuration described above, which in the context of the AdS_3/CFT_2 correspondence is expressed as follows

$$\mathcal{E} = \frac{3}{16G_N^{(3)}} (\mathcal{L}_{A_1} + \mathcal{L}_{A_2} - \mathcal{L}_{A_1 \cup A_2}). \quad (2.6)$$

Here $G_N^{(3)}$ is the $(2+1)$ -dimensional Newton constant and \mathcal{L}_{A_i} is the geodesic length anchored on the interval A_i . Using the Ryu-Takayanagi conjecture [3, 4] the Eq. (2.6) reduces to the following

$$\mathcal{E} = \frac{3}{4} (S_{A_1} + S_{A_2} - S_{A_1 \cup A_2}) = \frac{3}{4} [\mathcal{I}(A_1, A_2)], \quad (2.7)$$

which is precisely the mutual information between the subsystems described by the intervals A_1 and A_2 .

In the AdS_3/CFT_2 scenario being considered here, the bulk dual of the CFT_{1+1} at zero temperature is described by the AdS_3 vacuum, whose metric is given as follows

$$ds^2 = - \left(\frac{r^2}{R^2} \right) dt^2 + \left(\frac{r^2}{R^2} \right)^{-1} dr^2 + \left(\frac{r^2}{R^2} \right) d\phi^2, \quad (2.8)$$

where R is the radius of the AdS_3 space time. Employing the conjecture described above [22] the holographic entanglement negativity of the configuration in Fig. (2) may now be obtained as

$$\mathcal{E} = \frac{3R}{8G_N^{(3)}} \ln \left(\frac{l_1 l_2}{(l_1 + l_2)a} \right). \quad (2.9)$$

Remarkably the holographic entanglement negativity exactly reproduces the CFT_{1+1} result given in Eq. (2.5) in the large central charge limit [22, 23] upon using the Brown-Henneaux formula $c = \frac{3R}{2G_N^{(3)}}$ [24].

2.2 Entanglement negativity for two adjacent intervals at finite temperature

For the finite temperature case the entanglement negativity for the mixed state described by the configuration in Fig. (2) in the context of CFT_{1+1} may be obtained from Eq. (2.4) through the conformal map $z \rightarrow w = \frac{\beta}{2\pi} \ln z$ to the cylinder of circumference β . This leads to the following expression for the entanglement negativity

$$\mathcal{E} = \frac{c}{4} \ln \left(\frac{\beta}{\pi a} \frac{\sinh(\frac{\pi l_1}{\beta}) \sinh(\frac{\pi l_2}{\beta})}{\sinh(\frac{\pi(l_1+l_2)}{\beta})} \right) + \text{const}, \quad (2.10)$$

where $\beta = 1/T$ and a are the inverse temperature and the UV cut-off in the boundary field theory respectively. As earlier in the large central charge limit the ‘const’ term in the above equation may be neglected [22, 23].

The bulk dual for the above case is described by the $(2+1)$ dimensional Euclidean BTZ black hole whose metric is

$$ds^2 = \frac{(r^2 - r_+^2)}{R^2} d\tau^2 + \frac{R^2}{(r^2 - r_+^2)} dr^2 + \frac{r^2}{R^2} d\phi^2. \quad (2.11)$$

Here the horizon radius r_+ is related to the inverse Hawking temperature as $\beta = 2\pi R^2/r_+$. The holographic entanglement negativity for the two adjacent intervals at a finite temperature may then be obtained from the conjecture Eq. (2.6) proposed in [22]. Interestingly as earlier this exactly reproduces the finite temperature CFT_{1+1} result given by Eq. (2.10) in the large central charge limit upon using the Brown-Henneaux formula.

3 Holographic entanglement negativity for AdS_{d+1}/CFT_d

In this section we establish the holographic entanglement negativity conjecture for a mixed state described by two adjacent subsystems in a boundary CFT_d in the context of the AdS_{d+1}/CFT_d scenario which was alluded to in the article [22]. As mentioned in the Introduction this would involve an algebraic sum of the areas of the bulk co-dimension two extremal surfaces anchored on the respective subsystems. From the conjecture described in [22] the holographic entanglement negativity may then be expressed as follows

$$\mathcal{E} = \frac{3}{16G_N^{(3)}}(\mathcal{A}_1 + \mathcal{A}_2 - \mathcal{A}_{12}), \quad (3.1)$$

where \mathcal{A}_i is the extremal area of the co-dimension two surface anchored on the subsystem A_i . Using the Ryu-Takayanagi prescription [3, 4], it is possible to express the holographic entanglement negativity in the following form

$$\mathcal{E} = \frac{3}{4}(S_{A_1} + S_{A_2} - S_{A_1 \cup A_2}) = \frac{3}{4}[\mathcal{I}(A_1, A_2)], \quad (3.2)$$

where S_{A_i} is the holographic entanglement entropy of the subsystem A_i . Interestingly the expression in Eq. (3.2) is the holographic mutual information between the two adjacent subsystems modulo a constant factor. We are now ready to employ our holographic conjecture to evaluate the entanglement negativity for two adjacent subsystems described by $(d-1)$ -dimensional spatial rectangular strip geometries in the boundary CFT_d which we will describe in the subsequent sections.

4 Holographic entanglement negativity for AdS_{d+1}/CFT_d in vacuum

As mentioned above in this section we now proceed to the computation of the holographic entanglement negativity for two adjacent subsystems described by rectangular strip geometries in the boundary CFT_d at zero temperature. The corresponding bulk dual geometry in this case is the AdS_{d+1} vacuum space time whose metric in the Poincare coordinates is given as

$$ds^2 = \frac{1}{z^2} \left(-dt^2 + \sum_{i=1}^{d-1} dx_i^2 + dz^2 \right), \quad (4.1)$$

where the AdS radius has been set to $R = 1$. The respective rectangular strip geometries of the two subsystems A_1 and A_2 depicted in Fig. (3) are then specified as follows

$$x = x^1 \equiv \left[-\frac{l_j}{2}, \frac{l_j}{2}\right] \quad x^i = \left[-\frac{L}{2}, \frac{L}{2}\right], \quad i = 2, \dots, (d-1), \quad j = 1, 2. \quad (4.2)$$

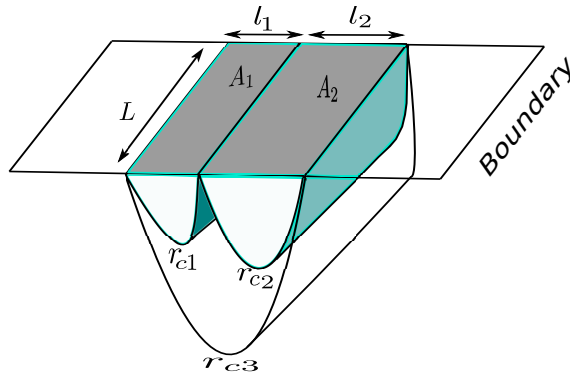


Figure 3: Schematic of the extremal surfaces that are anchored on the subsystems A_1 , A_2 and $A_1 \cup A_2$ involved in the computation of the holographic entanglement negativity of the adjacent subsystems in the boundary CFT_d .

We now briefly describe the computation for the areas of bulk co-dimension two extremal surfaces anchored on rectangular strip geometries in the boundary CFT_d [4]. The corresponding area functional

is expressed in the following way

$$\mathcal{A} = L^{d-2} \int_{-l/2}^{l/2} dx \frac{\sqrt{1 + (\frac{dz}{dx})^2}}{z^{d-1}}. \quad (4.3)$$

The Euler-Lagrange equation for the extremization problem is then given as

$$\frac{dz}{dx} = \frac{\sqrt{z_*^{2(d-1)} - z^{2(d-1)}}}{z^{d-1}}, \quad (4.4)$$

where $z = z_*$ is the turning point of the extremal surface. The extremal area may then be described as

$$\mathcal{A} = \frac{2}{d-2} \left(\frac{L}{a} \right)^{d-2} - 2I \left(\frac{L}{z_*} \right)^{d-2}, \quad (4.5)$$

where a is the UV cutoff and the constant I is given as

$$I = \frac{1}{d-2} - \int_0^1 \frac{dy}{y^{d-1}} \left(\frac{1}{\sqrt{1-y^{2(d-1)}}} - 1 \right) = -\frac{\sqrt{\pi} \Gamma\left(\frac{2-d}{2(d-1)}\right)}{\Gamma\left(\frac{1}{2(d-1)}\right)}. \quad (4.6)$$

Using the Eq. (4.5) and Eq. (4.6) it is now possible to express the area of the extremal co-dimension two surface as

$$\mathcal{A} = \mathcal{A}_{div} - \frac{2^{d-1}\pi^{(d-1)/2}}{d-2} \left(\frac{\Gamma\left(\frac{d}{2(d-1)}\right)}{\Gamma\left(\frac{1}{2(d-1)}\right)} \right)^{d-1} \left(\frac{L}{l} \right)^{d-2}, \quad (4.7)$$

where the divergent part \mathcal{A}_{div} of the area is

$$\mathcal{A}_{div} = \frac{2}{d-2} \left(\frac{L}{a} \right)^{d-2}. \quad (4.8)$$

One may now determine the holographic entanglement negativity \mathcal{E} for the mixed state at zero temperature in the boundary CFT_d described by the two strip geometries in Fig. (3) to be as follows

$$\mathcal{E} = \frac{1}{4G_N^{(d+1)}} \left[\frac{2}{d-2} \left(\frac{L}{a} \right)^{d-2} - \frac{2^{d-1}\pi^{(d-1)/2}}{d-2} \left(\frac{\Gamma\left(\frac{d}{2(d-1)}\right)}{\Gamma\left(\frac{1}{2(d-1)}\right)} \right)^{d-1} \left\{ \left(\frac{L}{l_1} \right)^{d-2} + \left(\frac{L}{l_2} \right)^{d-2} - \left(\frac{L}{l_1 + l_2} \right)^{d-2} \right\} \right]. \quad (4.9)$$

The first term in the above expression is the divergent term which is proportional to the area of the entangling surface between the two spatial strips on the d dimensional boundary and the second term describes the finite part of the negativity.

5 Holographic entanglement negativity for AdS_{d+1}/CFT_d at finite temperature

At finite temperatures the boundary CFT_d is dual to the AdS_{d+1} -Schwarzschild black hole with the following metric where the AdS -radius has been set to $R = 1$

$$ds^2 = -r^2 \left(1 - \frac{r_h^d}{r^d} \right) dt^2 + \frac{dr^2}{r^2 \left(1 - \frac{r_h^d}{r^d} \right)} + r^2 d\vec{x}^2. \quad (5.1)$$

The horizon radius r_h is related to the Hawking temperature as $T = r_h d / 4\pi$ and $\vec{x} \equiv (x, x^i)$ are the coordinates on the boundary. We first briefly review the computation for the area \mathcal{A} of the bulk AdS_{d+1} co-dimension two extremal surface anchored on a single rectangular strip on the boundary as described in [9]. This will be subsequently employed to compute the holographic entanglement negativity for the

configuration Fig. (3) in question. The extremal area functional anchored on a single rectangular strip is given as

$$\mathcal{A} = L^{d-2} \int dr r^{d-2} \sqrt{r^2 x'^2 + \frac{1}{r^2(1 - \frac{r_h^d}{r^d})}}. \quad (5.2)$$

The corresponding Euler-Lagrange equation for the extremization problem leads to the following

$$\frac{l}{2} = \frac{1}{r_c} \int_0^1 \frac{u^{d-1} du}{\sqrt{(1 - u^{2d-2})}} (1 - \frac{r_h^d}{r_c^d} u^d)^{-\frac{1}{2}}, \quad u = \frac{r_c}{r}, \quad (5.3)$$

where r_c as earlier describes the turning point. The area functional in terms of the variable u may now be expressed as follows

$$\mathcal{A} = 2L^{d-2} r_c^{d-2} \int_0^1 \frac{du}{u^{d-1} \sqrt{(1 - u^{2d-2})}} (1 - \frac{r_h^d}{r_c^d} u^d)^{-\frac{1}{2}}. \quad (5.4)$$

This leads us to the final expression for the area functional as

$$\mathcal{A} = (\mathcal{A}_{div} + \mathcal{A}_{finite}), \quad (5.5)$$

where \mathcal{A}_{div} is the temperature independent divergent part and \mathcal{A}_{finite} is the finite part. These may be expressed as follows

$$\begin{aligned} \mathcal{A}_{div} &= \frac{2}{d-2} \left(\frac{L}{a} \right)^{d-2}, \\ \mathcal{A}_{finite} &= 2L^{d-2} r_c^{d-2} \left[\frac{\sqrt{\pi} \Gamma\left(-\frac{d-2}{2(d-1)}\right)}{2(d-1) \Gamma\left(\frac{1}{2(d-1)}\right)} + \sum_{n=1}^{\infty} \left(\frac{1}{2(d-1)} \right) \frac{\Gamma\left(n + \frac{1}{2}\right) \Gamma\left(\frac{d(n-1)+2}{2(d-1)}\right)}{\Gamma(1+n) \Gamma\left(\frac{dn+1}{2(d-1)}\right)} \left(\frac{r_h}{r_c} \right)^{nd} \right]. \end{aligned} \quad (5.6)$$

Note that $r_c > r_h$ from [25] ensuring the convergence of the series in \mathcal{A}_{finite} . The holographic entanglement negativity for the mixed state described by the two intervals in the boundary CFT_d (Fig. (3)) may then be obtained from our conjecture Eq. (3.1) as

$$\begin{aligned} \mathcal{E} &= \frac{3}{16G_N^{(d+1)}} \left[\frac{2}{d-2} \left(\frac{L}{a} \right)^{d-2} \right. \\ &+ 2L^{d-2} r_{c1}^{d-2} \left\{ \frac{\sqrt{\pi} \Gamma\left(-\frac{d-2}{2(d-1)}\right)}{2(d-1) \Gamma\left(\frac{1}{2(d-1)}\right)} + \sum_{n=1}^{\infty} \left(\frac{1}{2(d-1)} \right) \frac{\Gamma\left(n + \frac{1}{2}\right) \Gamma\left(\frac{d(n-1)+2}{2(d-1)}\right)}{\Gamma(1+n) \Gamma\left(\frac{dn+1}{2(d-1)}\right)} \left(\frac{r_h}{r_{c1}} \right)^{nd} \right\} \\ &+ 2L^{d-2} r_{c2}^{d-2} \left\{ \frac{\sqrt{\pi} \Gamma\left(-\frac{d-2}{2(d-1)}\right)}{2(d-1) \Gamma\left(\frac{1}{2(d-1)}\right)} + \sum_{n=1}^{\infty} \left(\frac{1}{2(d-1)} \right) \frac{\Gamma\left(n + \frac{1}{2}\right) \Gamma\left(\frac{d(n-1)+2}{2(d-1)}\right)}{\Gamma(1+n) \Gamma\left(\frac{dn+1}{2(d-1)}\right)} \left(\frac{r_h}{r_{c2}} \right)^{nd} \right\} \\ &\left. - 2L^{d-2} r_{c3}^{d-2} \left\{ \frac{\sqrt{\pi} \Gamma\left(-\frac{d-2}{2(d-1)}\right)}{2(d-1) \Gamma\left(\frac{1}{2(d-1)}\right)} + \sum_{n=1}^{\infty} \left(\frac{1}{2(d-1)} \right) \frac{\Gamma\left(n + \frac{1}{2}\right) \Gamma\left(\frac{d(n-1)+2}{2(d-1)}\right)}{\Gamma(1+n) \Gamma\left(\frac{dn+1}{2(d-1)}\right)} \left(\frac{r_h}{r_{c3}} \right)^{nd} \right\} \right]. \end{aligned} \quad (5.7)$$

Here r_{c1}, r_{c2}, r_{c3} are the turning points of the extremal surfaces in the bulk anchored on the strips A_1, A_2 and $A_1 \cup A_2$ on the boundary respectively. It is required to evaluate the quantity r_{ci} from the Eq. (5.3) in terms of l_i and r_h . The corresponding integral is not analytically solvable but may be determined perturbatively for low and high temperature approximations described in the following subsections.

5.1 Entanglement negativity in the low temperature limit

At low temperature we have $Tl \ll 1$ ($r_h l \ll 1$) and r_c may be determined perturbatively as an expansion in $r_h l$ [9], which leads to the finite part of the area (5.6) as

$$\mathcal{A}_{finite} = s_0 \left(\frac{L}{l} \right)^{d-2} \left[1 + s_1 (r_h l)^d + O[(r_h l)^{2d}] \right]. \quad (5.8)$$

Here the constants s_0 and s_1 are given as

$$s_0 = \frac{2^{d-2} \pi^{\frac{d-1}{2}} \Gamma\left(-\frac{d-2}{2(d-1)}\right) \left(\Gamma\left(\frac{d}{2(d-1)}\right)\right)^{d-2}}{(d-1) \left(\Gamma\left(\frac{1}{2(d-1)}\right)\right)^{d-1}}, \quad (5.9)$$

$$s_1 = \frac{\Gamma\left(\frac{1}{2(d-1)}\right)^{d+1}}{2^{d+1} \pi^{\frac{d}{2}} \Gamma\left(\frac{d}{2(d-1)}\right)^d \Gamma\left(\frac{d+1}{2(d-1)}\right)} \left(\frac{\Gamma\left(\frac{1}{d-1}\right)}{\Gamma\left(-\frac{d-2}{2(d-1)}\right)} + \frac{2^{\frac{1}{d-1}} (d-2) \Gamma\left(1 + \frac{1}{2(d-1)}\right)}{\sqrt{\pi} (d+1)} \right).$$

The holographic entanglement negativity at low temperature for the mixed state in the boundary CFT_d described by the configuration in Fig (4) may now be obtained from our conjecture (3.1) and the Eqns (5.8) and (5.9) in the following way

$$\mathcal{E} = \frac{2}{d-2} \left(\frac{L}{a}\right)^{d-2} + \left[s_0 \left\{ \left(\frac{L}{l_1}\right)^{d-2} + \left(\frac{L}{l_2}\right)^{d-2} - \left(\frac{L}{l_1+l_2}\right)^{d-2} \right\} - k l_1 l_2 L^{d-2} T^d + s_0 \left\{ \left(\frac{L}{l_1}\right) \mathcal{O}(T l_1)^{2d} + \left(\frac{L}{l_2}\right) \mathcal{O}(T l_2)^{2d} \right\} \right]. \quad (5.10)$$

Here the constant k is given as

$$k = 2 \left(\frac{4\pi}{d}\right)^d s_0 s_1. \quad (5.11)$$

Note that the first and the second term in the above expression are temperature independent describing the contribution to the holographic entanglement negativity from the AdS vacuum Eq. (4.9). The remaining terms are the finite temperature corrections to the holographic entanglement negativity at low temperatures for the boundary CFT_d .

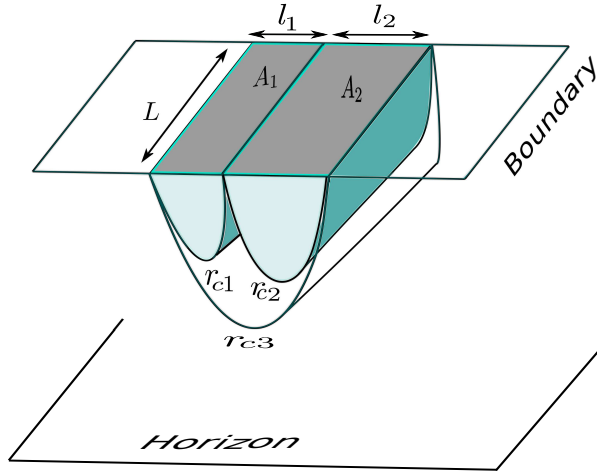


Figure 4: Schematic of the extremal surfaces that are anchored on the subsystems A_1 , A_2 and $A_1 \cup A_2$ in the boundary CFT_d at low temperatures.

5.2 Entanglement negativity in the high temperature limit

For high temperatures we have $Tl \gg 1$ ($r_h l \gg 1$) and in this case it is possible to obtain the quantity r_c Eq. (5.3) in a near horizon expansion in $\epsilon = (\frac{r_c}{r_h} - 1)$ [9] as follows

$$r_c = r_h (1 + \epsilon). \quad (5.12)$$

Here ϵ is expressed as

$$\epsilon = C_1 \exp\left(-\sqrt{\frac{d(d-1)}{2}} l r_h\right), \quad (5.13)$$

where the constant C_1 is given as

$$C_1 = \frac{1}{d} \exp \left[\sqrt{\frac{d(d-1)}{2}} \left\{ \frac{2\sqrt{\pi}\Gamma\left(\frac{d}{2(d-1)}\right)}{\Gamma\left(\frac{1}{2(d-1)}\right)} + 2 \sum_{n=1}^{\infty} \left(\frac{1}{1+nd} \frac{\Gamma\left(\frac{1}{2}+n\right)\Gamma\left(\frac{d(n+1)}{2(d-1)}\right)}{\Gamma(1+n)\Gamma\left(\frac{dn+1}{2(d-1)}\right)} - \frac{1}{\sqrt{2d(d-1)} n} \right) \right\} \right]. \quad (5.14)$$

The area of the extremal surface at high temperatures is expressed as

$$\mathcal{A} = \frac{2}{d-2} \left(\frac{L}{a} \right)^{d-2} + \left(\frac{4\pi}{d} \right)^{d-1} \left[V T^{d-1} + \frac{C_2}{8\pi} A' T^{d-2} - \frac{C_1}{8\pi} \sqrt{2d(d-1)} A' T^{d-2} \exp \left\{ -\sqrt{(d-1)/2d} 4\pi T l \right\} + \dots \right], \quad (5.15)$$

where $V = l L^{d-2}$ and $A' = 2L^{d-2}$ are the volume and area of a single strip respectively. The constant term C_2 is given as

$$C_2 = 2 \left[-\frac{\sqrt{\pi}(d-1)\Gamma\left(\frac{d}{2(d-1)}\right)}{(d-2)\Gamma\left(\frac{1}{2(d-1)}\right)} + \sum_{n=1}^{\infty} \frac{1}{1+nd} \left(\frac{d-1}{d(n-1)+2} \right) \frac{\Gamma\left(n+1/2\right)\Gamma\left(\frac{d(n+1)}{2d-2}\right)}{\Gamma(n+1)\Gamma\left(\frac{dn+1}{2d-2}\right)} \right]. \quad (5.16)$$

The holographic entanglement negativity at high temperatures for the mixed state in the boundary CFT_d described by the configuration in Fig. (5) may then be established from the Eq. (5.15) employing our conjecture as follows

$$\begin{aligned} \mathcal{E} = & \frac{1}{4G_N^{(d+1)}} \frac{2}{(d-2)} \left(\frac{A}{a^{d-2}} \right) + \frac{1}{4G_N^{(d+1)}} \left(\frac{4\pi}{d} \right)^{d-1} \left[\frac{C_2}{4\pi} A T^{d-2} \right. \\ & - \frac{C_1}{4\pi} \sqrt{2d(d-1)} A T^{d-2} \left\{ \exp \left(-\sqrt{(d-1)/2d} 4\pi T l_1 \right) + \exp \left(-\sqrt{(d-1)/2d} 4\pi T l_2 \right) \right. \\ & \left. \left. - \exp \left(-\sqrt{(d-1)/2d} 4\pi T (l_1 + l_2) \right) \right\} + \dots \right], \end{aligned} \quad (5.17)$$

where the ellipsis represent the higher order corrections and $A = L^{d-2}$ is the area of the entangling surface shared by the two adjacent strips on the boundary. Interestingly in the above expression notice that the thermal contribution to the holographic entanglement negativity (proportional to the volume in the Eq. (5.15)) has been subtracted out rendering it to be proportional to the area of the entangling surface. This is in conformity with the usual expectations from quantum information theory.

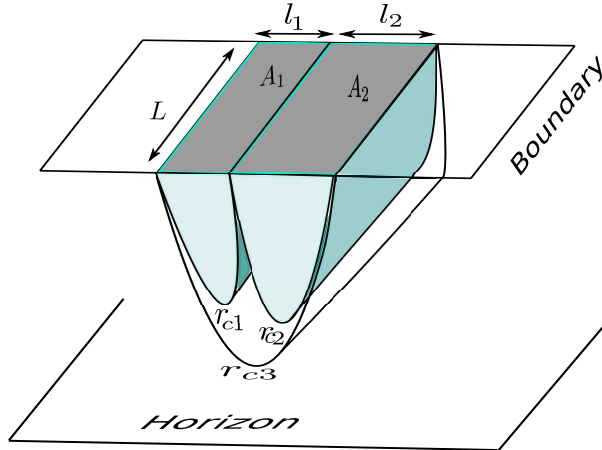


Figure 5: Schematic of the extremal surfaces that are anchored on the subsystems A_1 , A_2 and $A_1 \cup A_2$ in the boundary CFT_d at high temperatures.

6 Summary and conclusions

To summarize we have established a holographic conjecture for the entanglement negativity of mixed states described by two adjacent subsystems in a boundary CFT_d for both zero and finite temperatures. The corresponding subsystems are described by $(d - 1)$ -dimensional spatial rectangular strip geometries at the boundary in a AdS_{d+1}/CFT_d scenario. Our holographic prescription involves a certain algebraic sum of the areas of bulk co dimension two extremal surfaces anchored on the corresponding subsystems on the AdS_{d+1} boundary and was motivated by the corresponding analysis for the AdS_3/CFT_2 scenario in [22]. It is interesting that the algebraic sum described above actually characterizes the holographic mutual information between the two adjacent subsystems.

The holographic entanglement negativity for the boundary CFT_d at zero temperature could then be computed from the bulk dual configuration described by the AdS_{d+1} vacuum from our conjecture. The corresponding holographic entanglement negativity for the boundary CFT_d at finite temperature however involved a bulk dual configuration described by the AdS_{d+1} -Schwarzschild black hole with a planar horizon. In the latter case the area integrals were not analytically solvable and were evaluated in a perturbative expansion for low and high temperatures. It is observed from our computation that the leading contribution to the holographic entanglement negativity at low temperature arises from the AdS_{d+1} vacuum with subleading thermal corrections. Interestingly on the other hand at high temperatures the finite part of the holographic entanglement negativity is proportional to the area of the entangling surface on the boundary whereas the volume dependent thermal parts cancel out.

Our proposal provides a direct and elegant holographic prescription to compute the entanglement negativity of mixed states described by the specific configuration for boundary CFT_d both at zero and finite temperatures. It is well known from quantum information theory that the entanglement negativity characterizes the upper bound on the distillable entanglement for mixed states. It is expected that our conjecture will lead to a deeper understanding of entanglement issues for diverse applications of higher dimensional CFTs. It would be interesting to compute the holographic entanglement negativity for subsystems described by more general geometries other than the rectangular strip geometries considered by us. This would possibly lead to more exciting insights into the nature of holographic quantum entanglement and its relation to issues of quantum gravity. Naturally an explicit proof for our conjecture along the lines of the corresponding proof for the holographic entanglement entropy is an open issue that needs attention. We expect to return to these exciting issues in the near future.

7 Acknowledgment

Parul Jain would like to thank Prof. Mariano Cadoni for his guidance and the Department of Physics, Indian Institute of Technology Kanpur, India for their warm hospitality. Parul Jain's work is financially supported by Università di Cagliari, Italy and INFN, Sezione di Cagliari, Italy.

References

- [1] P. Calabrese and J. L. Cardy, “Entanglement entropy and quantum field theory,” *J. Stat. Mech.* **0406** (2004) P06002, [arXiv:hep-th/0405152](#) [[hep-th](#)].
- [2] P. Calabrese and J. Cardy, “Entanglement entropy and conformal field theory,” *J. Phys.* **A42** (2009) 504005, [arXiv:0905.4013](#) [[cond-mat.stat-mech](#)].
- [3] S. Ryu and T. Takayanagi, “Holographic derivation of entanglement entropy from AdS/CFT,” *Phys. Rev. Lett.* **96** (2006) 181602, [arXiv:hep-th/0603001](#) [[hep-th](#)].
- [4] S. Ryu and T. Takayanagi, “Aspects of Holographic Entanglement Entropy,” *JHEP* **08** (2006) 045, [arXiv:hep-th/0605073](#) [[hep-th](#)].
- [5] T. Takayanagi, “Entanglement Entropy from a Holographic Viewpoint,” *Class. Quant. Grav.* **29** (2012) 153001, [arXiv:1204.2450](#) [[gr-qc](#)].
- [6] T. Nishioka, S. Ryu, and T. Takayanagi, “Holographic Entanglement Entropy: An Overview,” *J. Phys.* **A42** (2009) 504008, [arXiv:0905.0932](#) [[hep-th](#)].
- [7] M. Cadoni and M. Melis, “Entanglement entropy of ads black holes,” *Entropy* **12** no. 11, (2010) 2244. <http://www.mdpi.com/1099-4300/12/11/2244>.
- [8] D. D. Blanco, H. Casini, L.-Y. Hung, and R. C. Myers, “Relative entropy and holography,” *Journal of High Energy Physics* **2013** no. 8, (2013) 60.

- [9] W. Fischler and S. Kundu, “Strongly Coupled Gauge Theories: High and Low Temperature Behavior of Non-local Observables,” *JHEP* **05** (2013) 098, [arXiv:1212.2643 \[hep-th\]](#).
- [10] W. Fischler, A. Kundu, and S. Kundu, “Holographic Mutual Information at Finite Temperature,” *Phys. Rev. D* **87** no. 12, (2013) 126012, [arXiv:1212.4764 \[hep-th\]](#).
- [11] P. Chaturvedi, V. Malvimat, and G. Sengupta, “Entanglement thermodynamics for charged black holes,” *Phys. Rev. D* **94** no. 6, (2016) 066004, [arXiv:1601.00303 \[hep-th\]](#).
- [12] G. Vidal and R. F. Werner, “Computable measure of entanglement,” *Phys. Rev. A* **65** (Feb, 2002) 032314. <http://link.aps.org/doi/10.1103/PhysRevA.65.032314>.
- [13] M. B. Plenio, “Logarithmic Negativity: A Full Entanglement Monotone That is not Convex,” *Phys. Rev. Lett.* **95** no. 9, (2005) 090503, [arXiv:quant-ph/0505071 \[quant-ph\]](#).
- [14] P. Calabrese, J. Cardy, and E. Tonni, “Entanglement negativity in extended systems: A field theoretical approach,” *J. Stat. Mech.* **1302** (2013) P02008, [arXiv:1210.5359 \[cond-mat.stat-mech\]](#).
- [15] P. Calabrese, J. Cardy, and E. Tonni, “Entanglement negativity in quantum field theory,” *Phys. Rev. Lett.* **109** (2012) 130502, [arXiv:1206.3092 \[cond-mat.stat-mech\]](#).
- [16] P. Calabrese, J. Cardy, and E. Tonni, “Finite temperature entanglement negativity in conformal field theory,” *J. Phys. A* **48** no. 1, (2015) 015006, [arXiv:1408.3043 \[cond-mat.stat-mech\]](#).
- [17] V. E. Hubeny, M. Rangamani, and T. Takayanagi, “A Covariant holographic entanglement entropy proposal,” *JHEP* **07** (2007) 062, [arXiv:0705.0016 \[hep-th\]](#).
- [18] M. Rangamani and M. Rota, “Comments on Entanglement Negativity in Holographic Field Theories,” *JHEP* **10** (2014) 060, [arXiv:1406.6989 \[hep-th\]](#).
- [19] P. Chaturvedi, V. Malvimat, and G. Sengupta, “Holographic Quantum Entanglement Negativity,” [arXiv:1609.06609 \[hep-th\]](#).
- [20] P. Chaturvedi, V. Malvimat, and G. Sengupta, “Covariant holographic entanglement negativity,” [arXiv:1611.00593 \[hep-th\]](#).
- [21] P. Chaturvedi, V. Malvimat, and G. Sengupta, “Entanglement negativity, Holography and Black holes,” [arXiv:1602.01147 \[hep-th\]](#).
- [22] P. Jain, V. Malvimat, S. Mondal, and G. Sengupta, “Holographic entanglement negativity conjecture for adjacent intervals in AdS_3/CFT_2 ,” [arXiv:1707.08293 \[hep-th\]](#).
- [23] M. Kulaxizi, A. Parnachev, and G. Policastro, “Conformal Blocks and Negativity at Large Central Charge,” *JHEP* **09** (2014) 010, [arXiv:1407.0324 \[hep-th\]](#).
- [24] J. D. Brown and M. Henneaux, “Central Charges in the Canonical Realization of Asymptotic Symmetries: An Example from Three-Dimensional Gravity,” *Commun. Math. Phys.* **104** (1986) 207–226.
- [25] V. E. Hubeny, “Extremal surfaces as bulk probes in AdS/CFT,” *JHEP* **07** (2012) 093, [arXiv:1203.1044 \[hep-th\]](#).